Chapter

Predictive Direct Torque Control Strategy for Doubly Fed Induction Machine for Torque and Flux Ripple Minimization

Gopala Venu Madhav and Y.P. Obulesu

Abstract

The main drawback of Direct Torque Control (DTC) or Direct Power Control (DPC) is non-constant switching frequency; this drawback can be eliminated by employing predictive DTC. The predictive DTC technique is employed without much complicated online calculations by simply implementing constant switching times for active rotor voltage vectors to reduce torque and flux ripples and achieve constant switching frequency. The predictive DTC strategy has been implemented for RSC of Doubly Fed Induction Machine (DFIM). The performance of the proposed control methodology is compared with the classical DTC method under various operating conditions such as step change in torque, continuous variation of torque command, and the performance of DFIM near synchronous speed. It is found that the performance of the proposed predictive DTC strategy of DFIM is quite good compared to classical DTC strategy.

Keywords: predictive direct torque control, classical direct torque control, doubly fed induction machine, torque ripple, flux ripple

1. Introduction

In the field of renewable energy sources, wind energy is gaining much importance. The increase in the level of generation has two main restrictions, one is due to the limitations of the switching frequency of the power devices with respect to the power drive of the Doubly Fed Induction Machine (DFIM) and second one is the requirement of good dynamic torque performance, these restrictions are addressed by the proposed new Direct Torque Control (DTC) approach.

The foremost torque control methods proposed were classified into Field Oriented Control (FOC) techniques, Blaschke [1] and the direct control techniques. Then after, the concept of DTC, Takahashi and Ohmori [2] and Direct Self Control (DSC), Depenbrock [3] were introduced to achieve good steady-state and transient torque control conditions. Moreover, direct control techniques do not require current regulators, nor coordinate transformations or specific modulations like Pulse Width Modulation (PWM) or Space Vector Modulation (SVM) for pulse generation. The disadvantages are the lack of direct current control, torque control difficulties at very low speeds and especially variable switching frequency behavior.

The last important drawback put forward several authors in recent years, thus, methods like Direct Mean Torque Control (DMTC), [4] and Direct Torque Control based on Discrete Space Vector Modulation (DTC–DSVM), [5], have already achieved constant switching frequency. Furthermore, the methods proposed in Kang and Sul [6, 7] have extended the solution to reduce torque ripple at the same time imposing the switching frequency, as well as for different voltage-source multilevel topologies.

Further the concept of DTC have been applied to the brushless doubly fed induction machine, [8], or the equivalent Direct Power Control (DPC) strategy for several grid connected converter applications, [9].

In this paper, the analysis on the Doubly Fed Induction Machine (DFIM), which is a common solution for variable speed wind turbines, is discussed. The control methods like FOC have been performed by many authors, for example [10]. DTC and DPC methods without switching frequency imposition have also been carried out in Gomez & Amenedo [11], Datta & Ranganathan [12], while the DPC at constant switching frequency has also been developed in [13].

These mentioned direct control techniques that achieve constant switching frequency behavior are based on predictive control with a prediction horizon equal to one sample period. In this paper, predictive DTC technique for the DFIM will be employed based on [13] and the performance is compared with the DTC strategy, at constant switching frequency and with reduced torque and flux ripples criteria. This control technique is based on a prediction of the torque and the flux evolution of the DFIM. Hence, the new Predictive DTC (PDTC) strategy presented in this paper is based on a direct control of the electromagnetic torque and the rotor flux of the machine. Simulation results are presented and discussed, and at last, the results show that the predictive DTC technique presents good dynamic response compared to classical DTC concept.

In this Chapter, predictive DTC technique for the DFIM has been implemented and its performance is compared with the classical DTC of DFIM based on certain parameters like constant switching frequency, torque ripple and flux ripple. This control technique is based on a prediction of the torque and the flux evolution of the DFIM. To validate the proposed control scheme, results are presented. From these results, it is observed that the predictive DTC technique gives good dynamic response compared to classical DTC concept.

The control strategy even reduces the switching losses of the converter and reduces the electromagnetic torque and flux ripples at low switching frequency even under variable speed operating conditions.

In Section 1, the introduction of the Chapter is given.

In Section 2, Contributions and Novelty of this Chapter is explained.

In Section 3, Modeling of the DFIM is given.

In Section 4, the basic control principle of predictive DTC is explained and also implementation of the proposed predictive DTC strategy of DFIM along with selection of rotor voltage vectors for constant switching frequency and reduction of switching power losses are described.

In Section 5, Results are presented to validate the proposed control strategy.

In Section 6, the Conclusions of the Chapter are described.

In Section 7, the summary of the Chapter is given.

2. Contributions and novelty

The main contributions of this Chapter are as follows:

- Implementation of a new predictive Direct Torque Control (DTC) strategy of the Doubly Fed Induction Machine (DFIM) is presented which is designed to operate at a low constant switching frequency.

- The proposed DTC method effectively reduces the torque and flux ripples at low switching frequency, even under variable speed operation conditions.

- Results are presented to validate the proposed control strategy.

The novelty of this Chapter is that the predictive DTC have been developed to control the different parameters of DFIM, to improve its performance during transient, steady state, tracking behavior and operation near synchronous speed. All these cases are thoroughly investigated.

3. Modeling of DFIM

The DFIG model adopted is the qd0 rotating reference frame. It is because the model of DFIM is quite suitable with this frame of reference during transients. The transient solution of the DFIM model is possible because of the transformation from abc to qd0 by which the differential equations with time-varying inductances is converted into differential equations with constant inductances,

$$v_{qs} = R_s i_{qs} + \omega_s \psi_{ds} + \frac{d\psi_{qs}}{dt}$$
$$v_{ds} = R_s i_{ds} - \omega_s \psi_{qs} + \frac{d\psi_{ds}}{dt} \quad (1)$$

(or) simply (1) can be written as

$$\bar{v}_s^s = R_s \bar{i}_s^s + \frac{d\bar{\psi}_s^s}{dt} \quad (2)$$

Similarly, the q and d-axis rotor voltages referred to the stator are given by,

$$v'_{qr} = R'_r i'_{qr} + (\omega_s - \omega_r)\psi'_{dr} + \frac{d\psi'_{qr}}{dt}$$
$$v'_{dr} = R'_r i'_{dr} - (\omega_s - \omega_r)\psi'_{qr} + \frac{d\psi'_{dr}}{dt} \quad (3)$$

(or) simply (3) can be written as

$$\bar{v}_r^s = R_r \bar{i}_r^s + \frac{d\bar{\psi}_r^s}{dt} - j\omega_m \bar{\psi}_r^s \quad (4)$$

The stator and rotor fluxes can be calculated by using (5) and (6) can be used to calculate the magnitudes.

$$\begin{aligned}\bar{\Psi}_s &= L_s\bar{I}_s + L_m\bar{I}_r \\ \bar{\Psi}_r &= L_m\bar{I}_s + L_r\bar{I}_r\end{aligned} \tag{5}$$

$$|\psi_s| = \sqrt{\psi_{ds}^2 + \psi_{qs}^2} \tag{6}$$

$$|\psi_r| = \sqrt{\psi_{dr}^2 + \psi_{qr}^2}$$

The electromagnetic torque of DFIM is given in (7).

$$T_{em} = \frac{3}{2}p\mathrm{Im}\{\hat{\bar{\Psi}}_s.\bar{i}_s\}\,(\mathrm{or})\,\frac{3}{2}p\left(\psi_{s\alpha}i_{s\beta} - \psi_{s\beta}i_{s\alpha}\right) \tag{7}$$

$$(\mathrm{or})\,\frac{3}{2}p\left(\psi_{ds}i_{qs} - \psi_{qs}i_{ds}\right)(\mathrm{or}) \approx \frac{3}{2}\frac{p}{2}L_m(i'_{dr}i_{qs} - i'_{qr}i_{ds})$$

The active and reactive powers are given by:

$$P_s = \frac{3}{2}\mathrm{Re}\{\bar{v}.\hat{\vec{i}}\}\,(\mathrm{or})\,\frac{3}{2}\left(v_\alpha i_\alpha + v_\beta i_\beta\right)(\mathrm{or})\,\frac{3}{2}\left(v_d i_d + v_q i_q\right)\bar{\Psi}_r = L_m\bar{I}_s + L_r\bar{I}_r$$

$$Q_s = \frac{3}{2}\mathrm{Im}\{\vec{v}.\hat{\vec{i}}\}(\mathrm{or})\frac{3}{2}\left(v_\beta i_\alpha - v_\alpha i_\beta\right)(\mathrm{or})\frac{3}{2}\left(v_q i_d - v_d i_q\right) \tag{8}$$

4. Description of proposed predictive direct torque control strategy for torque and flux ripple minimization

The main drawback of classical DTC scheme is nonconstant switching behavior; it is avoided by the proposed predictive Direct Torque Control strategy. The constant switching behavior is achieved by increasing slightly the complexity of control strategy.

A sequence of three voltage vectors will be introduced at a constant switching period of which two are active vectors always followed by a zero vector, in order to reduce the ripples of both directly controlled variables compared to selection of four rotor voltage vectors depending on the position of rotor flux in classical DTC scheme. For that purpose, ripple reduction criteria based on a prediction of the electromagnetic torque and rotor flux evolution over time is implemented which is derived from (7) and (10) [13] and illustrated in **Figure 1(a)**.

The basic principles of the predictive DTC scheme are firstly, constant switching period 't_s' is defined. In predictive DTC, the control procedure is discretized unlike in DTC scheme, which is based on time domain. Secondly, at steady state condition, by taking the electromagnetic torque and flux amplitude errors to be minimized, the three different rotor voltage vectors are injected during t_s. Note that according to the chosen three vector sequence together with the specified time intervals for each vector, the electromagnetic torque and flux evolutions within the switching period can be different. Thirdly, this procedure is repeated at constant period t_s.

The Doubly Fed Induction Machine is modeled using (2), (4)–(6). The torque is calculated by using (7) in terms of complex conjugate of rotor flux and stator flux.

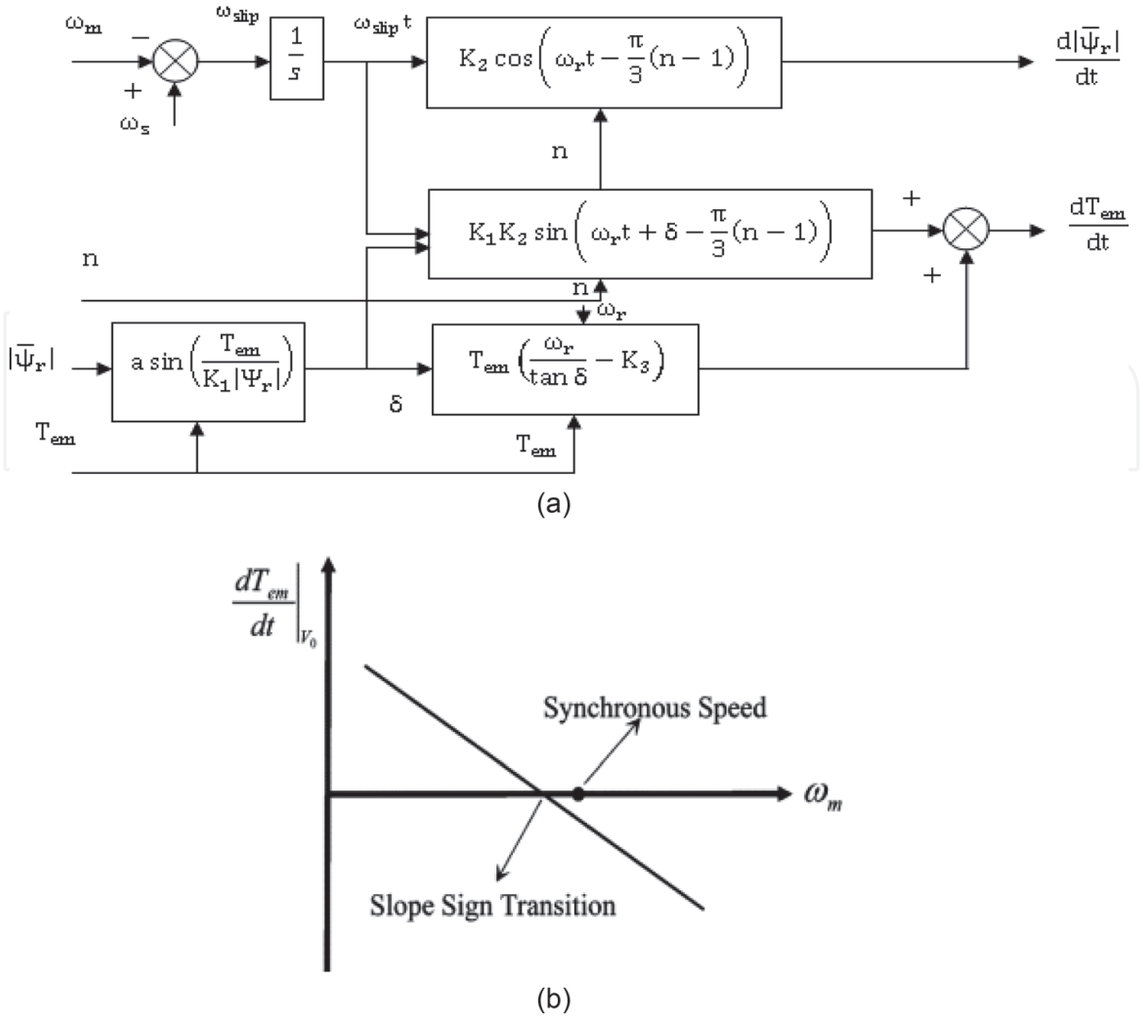

Figure 1.
(a) Simplified prediction scheme of torque and rotor flux of DFIM. (b) Variation of electromagnetic torque with zero vectors at constant torque and rotor flux.

4.1 Effect of voltage vector on the DFIM

Using (2), (4)–(7), the predictive expressions for torque and rotor flux are given by [2, 13]

$$\frac{d|\bar{\psi}_r|}{dt} = \frac{1}{|\bar{\psi}_r|}\left[\left(\frac{R_r L_m}{\sigma L_s L_r}\right) Re\{\bar{\psi}_r . \bar{\psi}_s\} - \left(\frac{R_r}{\sigma L_r}\right)|\bar{\psi}_r|^2 + Re\{\bar{\psi}_s . \bar{v}_r\}\right] \quad (9)$$

$$\frac{dT_{em}}{dt} = \frac{3}{2} p \frac{L_m}{\sigma L_s L_r}\left[\left(\frac{R_s}{\sigma L_s} + \frac{R_r}{\sigma L_r}\right) Im\{\bar{\psi}_r . \bar{\psi}_s^*\} - \omega_m Re\{\bar{\psi}_r . \bar{\psi}_s\} + Im\{\bar{v}_s . \bar{\psi}_r^*\} + Im\{\bar{\psi}_s . \bar{v}_r^*\}\right] \quad (10)$$

The below space vector representations are used in order to analyze the expressions (9) and (10).

$$\bar{\psi}_r = |\bar{\psi}_r| e^{j\omega_s t} \quad (11)$$

$$\bar{\psi}_s = |\bar{\psi}_s| e^{j(\omega_s t + \delta)} \quad (12)$$

$$\bar{v}_s = |\bar{v}_s| e^{j\left(\omega_s t + \left(\frac{\pi}{2}\right) + \delta\right)} \quad (13)$$

$$\bar{v}_r = \frac{2}{3} V_{DC} e^{j(\omega_m t + \pi/3(n-1))} \tag{14}$$

where n is representation of sectors from 0 to 7. In (9), if Eqs. (11)–(14) are substituted, then

$$\frac{d|\bar{\psi}_r|}{dt} = \left[\left(\frac{R_r L_m}{\sigma L_s L_r}\right)|\bar{\psi}_s| \cos\delta - \left(\frac{R_r}{\sigma L_r}\right)|\bar{\psi}_r| + \frac{2}{3} V_{DC} \cos\left(\omega_{slip} t - \frac{\pi}{3}(n-1)\right)\right] \tag{15}$$

where

$$\omega_{slip} = \omega_s - \omega_m \tag{16}$$

Eq. (15) comprises of a cosine term and two constant terms, the cosine term with depends on DC bus voltage and it indicates that the cosine term of rotor flux variation is constant for zero vectors and only depends on active vectors.

Eq. (10) can be simplified considering the stator flux vector module which is nearly constant.

$$\frac{dT_{em}}{dt} = T_{em}\left(\frac{\omega_{slip}}{\tan\delta} - \left(\frac{R_s}{\sigma L_s} + \frac{R_r}{\sigma L_r}\right)\right) + p\frac{L_m}{\sigma L_s L_r} V_{DC}|\bar{\psi}_s| \sin\left(\omega_{slip} t + \delta - \frac{\pi}{3}(n-1)\right) \tag{17}$$

Eq. (17) is similar to rotor flux derivation with only one constant and one sine term.

Equations (15) and (17) are used practically as shown in **Figure 1(a)**, instead of (9) and (10). As shown in **Figure 1(a)**, the torque and flux derivatives depends on only four terms when considering the DC bus voltage, stator voltage and flux as constant magnitudes. In the expression (17), the constant term depends on T_{em} and, that means it depends on machine operating condition, which can be positive or negative as shown in **Figure 1(b)**. Because of this reason only, the phase shift order of each active vector varies, whereas, it is not like that for rotor flux derivative. The key point is knowing the slopes or the derivatives of torque and flux for each of the rotor voltage vector based on **Figure 1(a)** and **Table 1** and considering these slopes to be constants within the specific time in the given switching period, t_s, the torque and flux ripples can be maintained within the limits.

With constant values

$$K_1 = \frac{3}{2} p \frac{L_m}{\sigma L_s L_r} |\bar{\psi}_s| \tag{18}$$

$$K_2 = \frac{2}{3} V_{DC} \tag{19}$$

$$K_3 = \frac{R_s}{\sigma L_s} + \frac{R_r}{\sigma L_r} \tag{20}$$

From the **Figure 1(b)**, it can be seen that the slope of torque derivative varies proportionally to the slip speed provided at fixed torque and rotor flux operating conditions and also near synchronous speed, the slope of the zero vector becomes smaller obeying the fact that from the expression (17) the zero vector produce small

torque variation. This fact implies that near synchronous speed the amplitude of rotor voltage vector is small demanding the condition of zero vectors. As shown in **Figure 1(b)**, this transition from positive to negative torque slope is different to the synchronous speed.

4.2 Selection of first rotor voltage vector

The first vector is selected depending on the errors of torque and flux and the sector where the rotor flux lies, the look up table for vector selection is shown in **Table 1**. From the **Table 1**, it is noticed that the required rotor voltage vector should produce either positive or negative slope variation depending on the output of the torque or flux hysteresis comparators that is either 1 or −1, respectively.

4.3 Selection of second and third vector rotor voltage vector

The first vector is actually selected based on the classical DTC; the second vector is selected such that it is always followed by zero vectors in order to reduce the torque and flux ripples based on the predictive DTC strategy.

From **Figure 2**, it can be seen that from the derivative calculations block the required values of torque and flux evolutions depending on the each rotor voltage selected are fed to the ripple reduction criteria block, in which based on the slopes calculations by (15) and (17), the required rotor voltage vectors which are selected are active for the time period of this constant slopes. This constant time period of the constant slopes is fed to the switching table, where in the switching operation of rotor voltages are chosen in such a way that it reduces the switching losses.

From (15) and (17), it can be inferred that the rotor flux is constant for zero vector and it produces opposite sign for torque variation for first two active vectors. These two active vectors along with zero vectors are useful to control torque and rotor flux. By the two active vectors the rotor flux as one vector produce positive slope, the other vectors produce negative slope because of this the flux ripple is not eliminated completely as compared to torque ripple and further it affects the rotor and stator currents. **Table 2** shows the selection of second active vector, after the first active vector is selected. It clearly shows that, one vector cannot be selected, as the flux would have a very big or small variation, which leads to poor quality of flux output.

4.4 Reduction of switching power losses

The right choice of zero vectors V_0 and V_7 implies that there is reduction in switching power loss of the converter. Two different switching sequences exist for each pair of required active vectors, which allows the commutations of the converter to be reduced. **Table 3** shows the correct sequence of vectors, which allows only four commutations per switching period t_s. The candidate sequences are such

		Error of electromagnetic torque	
		1	**−1**
Error value of rotor flux	1	$V_{(n-1)}$	$V_{(n+1)}$
	−1	$V_{(n-2)}$	$V_{(n+2)}$

n = sector.

Table 1.
Selection of voltage vectors [13].

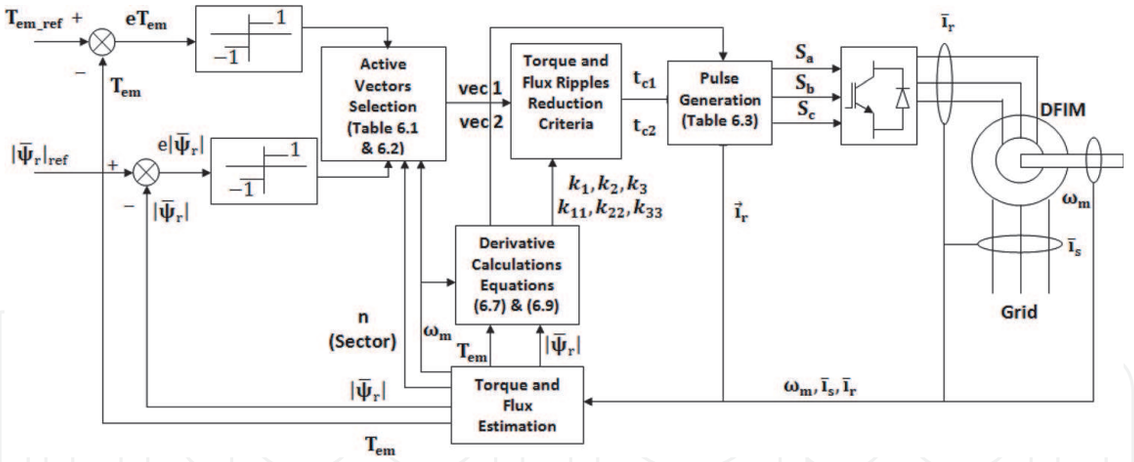

Figure 2.
Block diagram of proposed predictive direct torque control strategy of DFIM.

	Active vectors
Below synchronous speed	$V_{(n+1)}$, $V_{(n+2)}$
Above synchronous speed	$V_{(n-1)}$, $V_{(n-2)}$

n = sector.

Table 2.
Selection of active vectors under steady-state [13].

Active vectors	Sector	Switching sequences	Zero vector
V_1-V_2	6(subs)	100-110-111	V_7
	3(hypers)	110-100-000	V_0
V_2-V_3	1(subs)	110-010-000	V_0
	4(hypers)	010-110-111	V_7
V_3-V_4	2(subs)	010-011-111	V_7
	5(hypers)	011-010-000	V_0
V_4-V_5	3(subs)	011-001-000	V_0
	6(hypers)	001-011-111	V_7
V_5-V_6	4(subs)	001-101-111	V_7
	1(hypers)	101-001-000	V_0
V_6-V_1	5(subs)	101-100-000	V_0
	2(hypers)	100-101-111	V_7

subs – sub synchronous speed operation, hypers – super synchronous speed operation.

Table 3.
Sequence of vector selection for reduction of switching power losses under steady-state [13].

that it reduces the switching power losses by transmitting the smallest current values, which is the main task of the proposed control strategy.

5. Results and discussion

The predictive DTC control scheme of DFIM has been implemented using MATLAB/Simulink. The specifications of DFIM are given in **Table 4**. The

Doubly fed induction machine	
Specifications	**Ratings**
Rated power	2.6 MW
Rated voltage	690 V
Synchronous speed	1500 rpm
Frequency	50 Hz
Number of pairs of poles	2
Stator to rotor turns ratio	0.34
Base voltage	398.4 V
Base current	2175 A
Base angular frequency	157 $rads^{-1}$
Base power	2.6 MW
Stator resistance	0.0108 pu
Stator leakage inductance	0.102 pu
Magnetizing inductance	3.362 pu
Rotor resistance referred to stator	0.0121 pu
Rotor leakage inductance referred to stator	0.11 pu
Inertia constant(H)	0.5 s
Friction coefficient(F)	0.05479 pu
DC-link capacitance	5e–3F
DC-link voltage	1200 V
Wind turbine	
Number of blades	3
Rotor diameter	70 m
Hub height	84.3 m
Turbine total Inertia	4.4532 e5Kgm^2
Stiffness constant (B)	2 pu
Mutual damping	1.5 pu
Cut-in wind speed	3 ms^{-1}
Cut-out wind speed	25 ms^{-1}
Rated wind speed	15 ms^{-1}

Table 4.
Specifications of DFIM and wind turbine.

conditions of steady state, transient, tracking behavior, and performance near synchronism of DFIM are examined, which are given in three subsections.

5.1 Transient and steady state analysis of DFIM

The performance of proposed control strategy of DFIM is analyzed for steady state and transient conditions. For the transient conditions, the step change in electromagnetic torque i.e., from −0.4 pu to +0.4 pu at 0.6 s is considered. That means, from generator mode (negative torque) to motoring mode (positive torque), with constant switching frequency of 1 kHz, with speed reference of 1350 rev/min, and DC-link voltage of 1200 V. The DFIM is under steady state

operation up to 0.6 s with torque of −0.4 pu and at 0.6 s the DFIM enters into transient state, and again it reaches its steady state value of 0.4 pu.

The response of stator currents in stationary reference frame are shown in **Figure 3(a)**. Therefore, there are two waveforms which refer to α, β components of stator currents. From the **Figure 3(a)**, it is observed that there are no over currents in stator, which indicates the effectiveness of the proposed control scheme even at sudden variation in torque demand. This is possible because of selection of proper rotor voltage vectors with their respective time intervals.

Figure 3(b) shows the response of developed torque for the proposed strategy and classical DTC strategy (not expressed in p.u. value), from the figure, it is noticed that the torque response of the DFIM closely followed the torque command and also torque ripple is zero.

From the **Figure 3(c)**, it can be seen that stator active power has good dynamic response when the reference torque is changed suddenly. From the figure, it is observed that the stator active power follows the torque demand to make the DFIM to develop the torque to match its reference value.

The response of the stator flux is shown in **Figure 3(d)**, from the figure, it is clearly noticed that the stator flux response remains constant which is not affected by variation in torque command.

The response of the rotor flux is shown in **Figure 3(e)**, from the figure, it is observed that the rotor flux response is also not affected by change in reference torque and also the rotor flux response is sinusoidal in nature which is not distorted due to sudden change in torque command.

Figure 3(f) shows response of the rotor speed of DFIM. From the **Figure 3(f)**, it is observed that there is decrease in rotor speed due to step change in reference torque but decrease in rotor speed is very small.

The response of rotor currents is shown in **Figure 3(g)**. From the **Figure 3(g)**, it is observed that there are no over currents in rotor, which indicates the effectiveness of the proposed control scheme even at sudden variation in torque demand. This is possible because of selection of proper rotor voltage vectors with their respective time intervals.

5.2 Performance analysis of DFIM during variable torque behavior

In this section, the proposed control scheme of DFIM is investigated for variable speed operation implying wind energy applications, and at the same instant, the torque reference may also vary respectively with speed of DFIM. This kind of behavior of wind energy system is called as tracking behavior. At this condition, the actual values of the DFIM should follow the reference values as closely as possible and this is clearly guaranteed by proposed control strategy which can be seen clearly through the results presented in this section. To explore the tracking behavior of DFIM, sinusoidally varying reference torque with amplitude of 0.4 pu and frequency of 3 Hz is set to the DFIM. By this set reference torque, the DFIM operates in generating and motoring modes. In this mode of operation, the other parameters of DFIM are same as mentioned in Section 5.1.

The predictive DTC strategy has good tracking behavior and it is confirmed that the reduction in torque and flux ripples is achieved as there are absolute absence of over currents and reduced ripples in stator currents as shown in **Figure 4(a)**. From the **Figure 4(a)**, it is noticed that there is continuous increase and decrease in the amplitude of stator currents for maintaining the consistency due to variable behavior of torque command. The stationary reference frame stator currents are clearly noticed in **Figure 4(a)**.

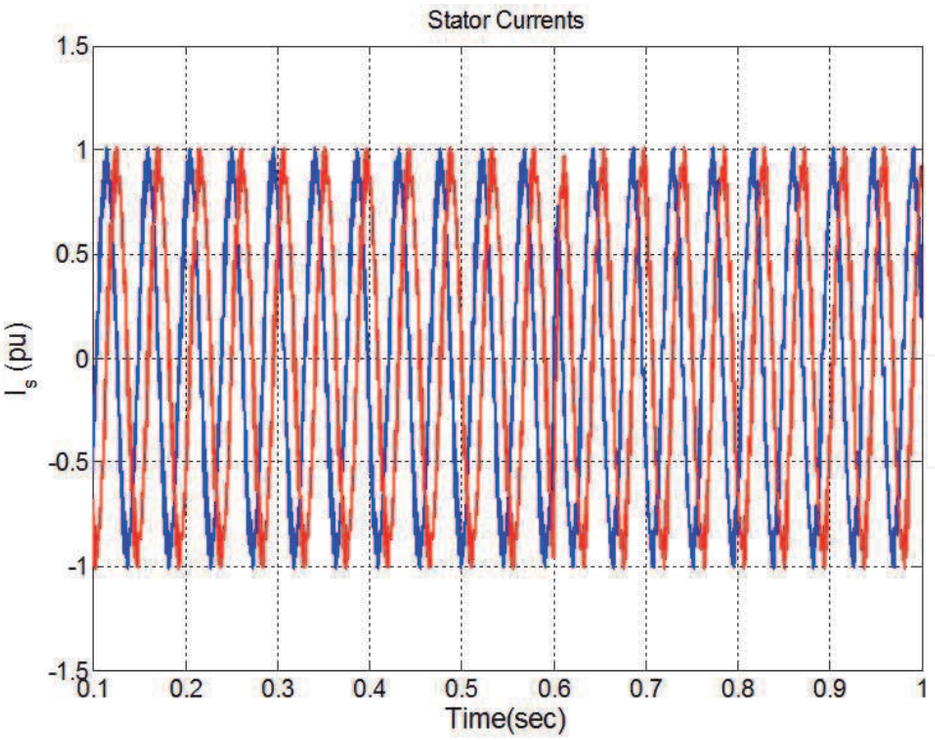
Stator Currents
I_s (pu)
Time(sec)

(a)

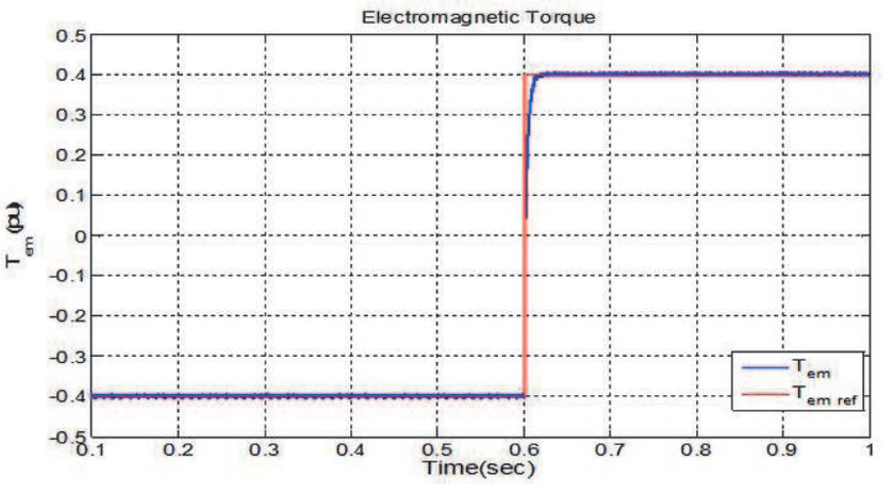
Electromagnetic Torque
T_{em} (pu)
Time(sec)
T_{em}
$T_{em\ ref}$

(i)

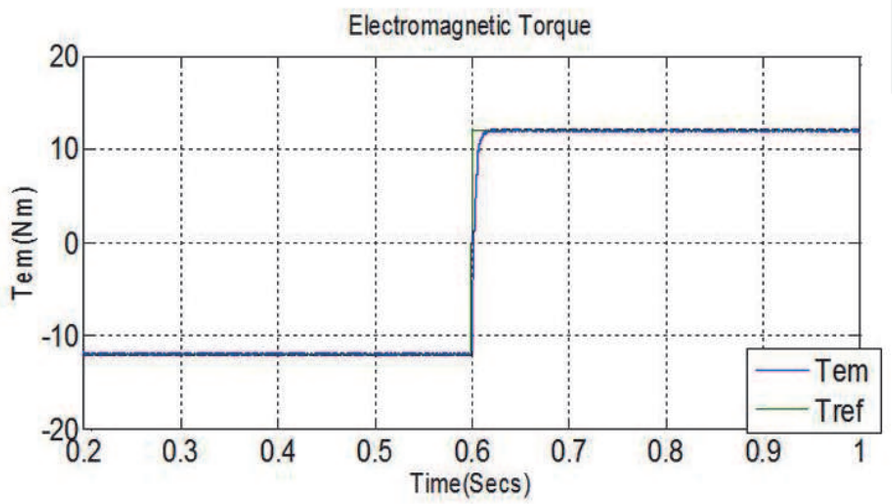
Electromagnetic Torque
Tem(Nm)
Time(Secs)
Tem
Tref

(ii)

(b)

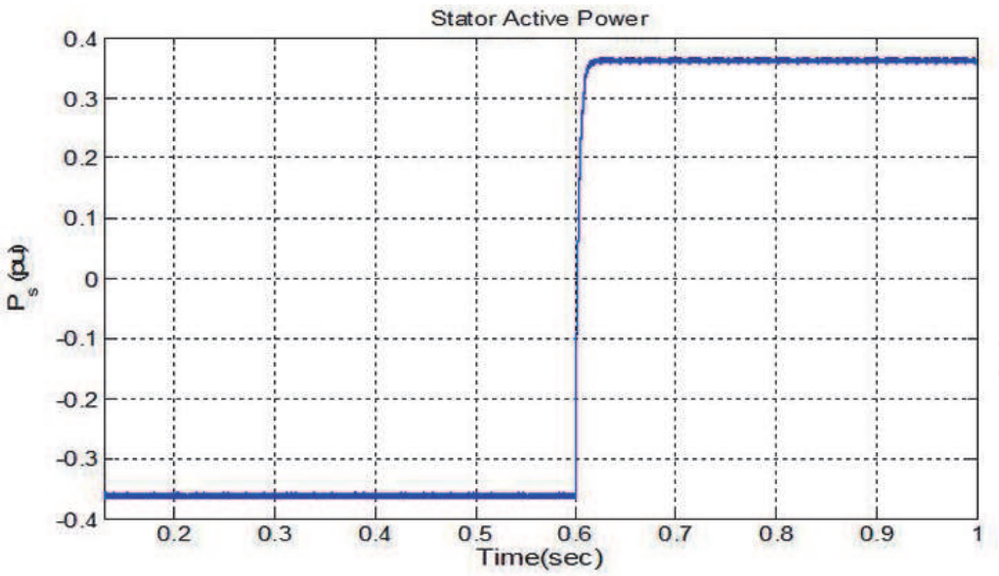
Stator Active Power
P_s (pu)
Time(sec)

(c)

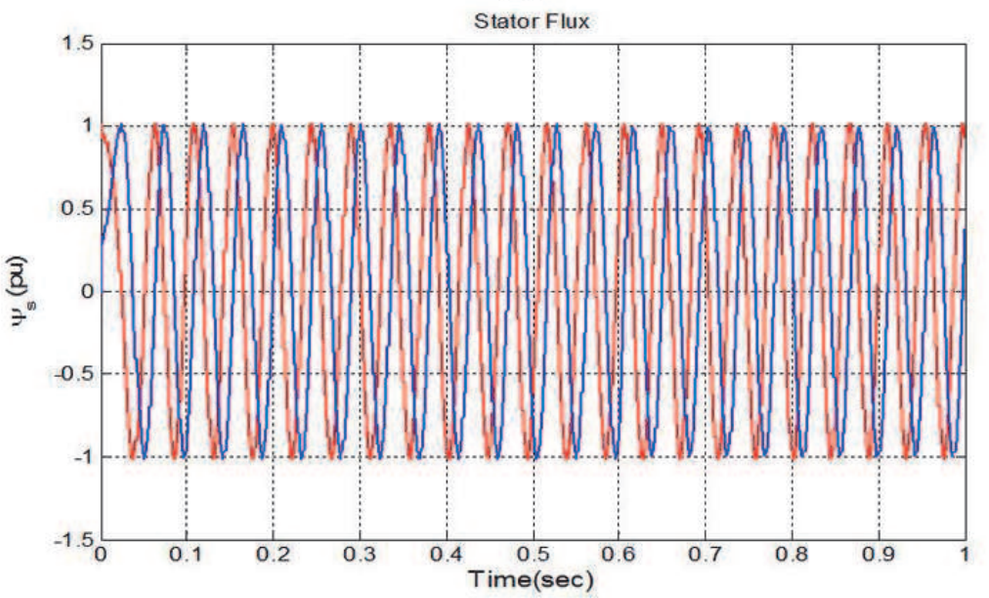
Stator Flux
ψ_s (pu)
Time(sec)

(d)

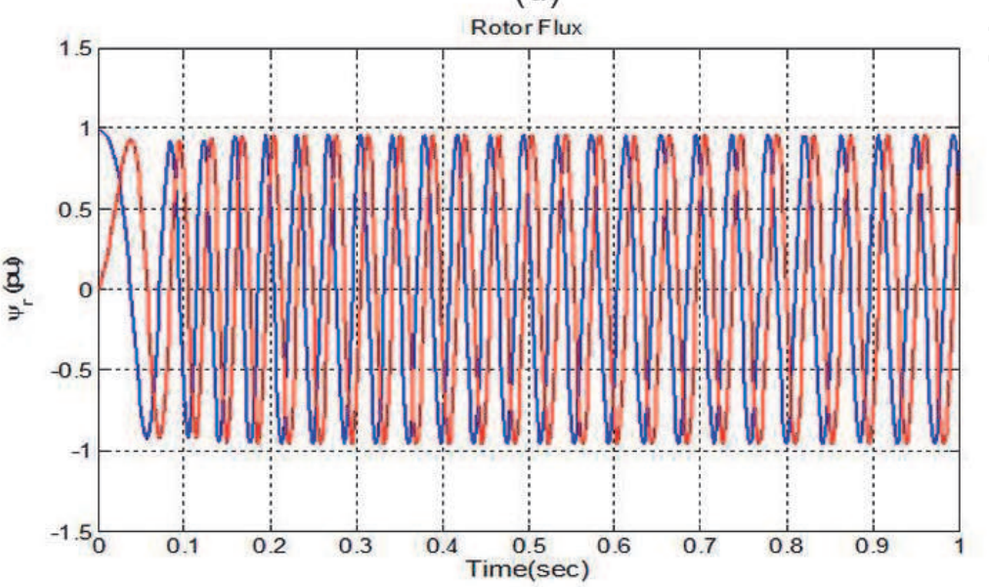
Rotor Flux
ψ_r (pu)
Time(sec)

(e)

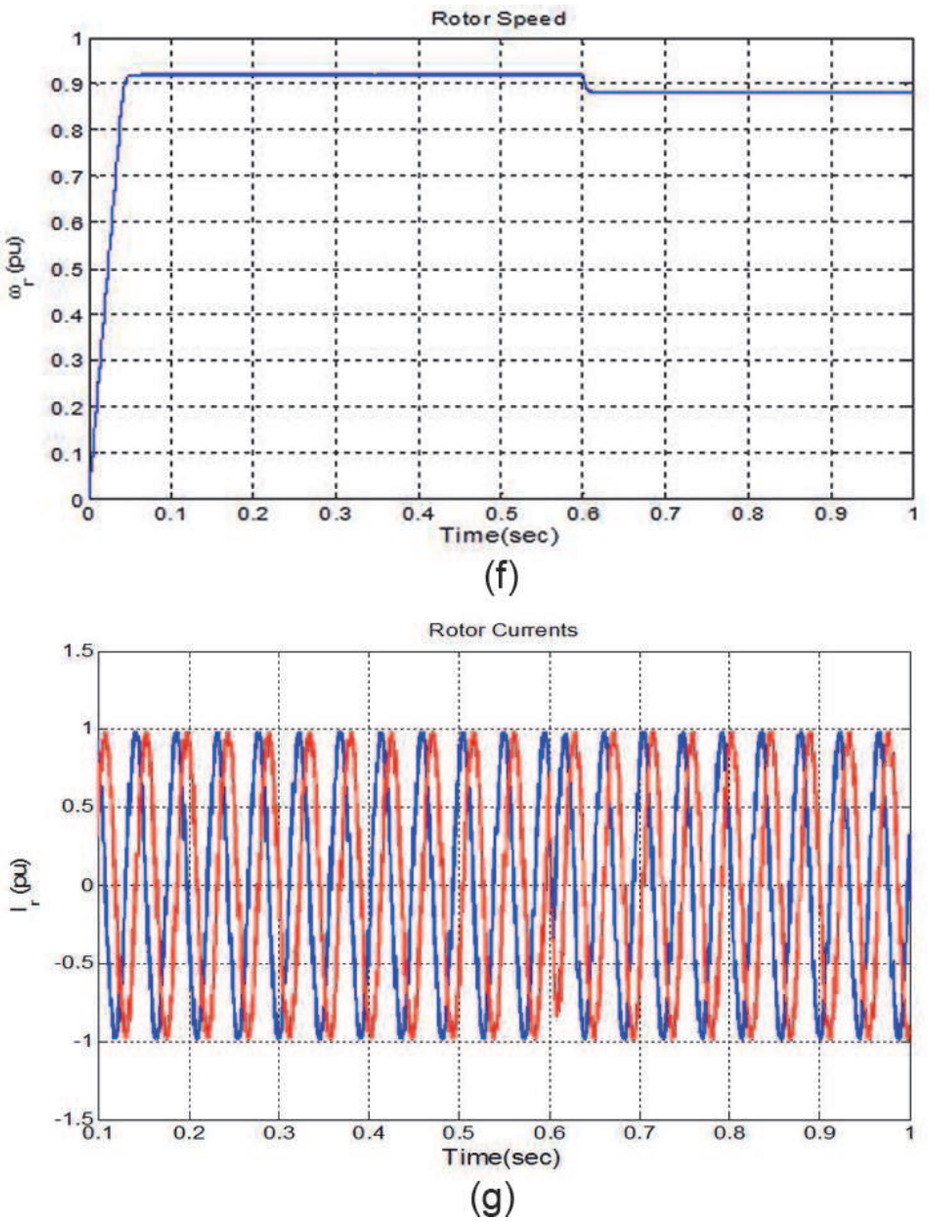

Figure 3.
(a) Response of stator currents of DFIM for step change in T_{em} from −0.4 pu to 0.4 pu at 0.6 s. (b) Torque response of DFIM for step change in T_{em} from −0.4 pu to 0.4 pu at 0.6 s, (i) proposed strategy (ii) classical DTC. (c) stator active power of DFIM for step change in T_{em} from −0.4 pu to 0.4 pu at 0.6 s. (d) Stator flux response of DFIM for step change in T_{em} from −0.4 pu to 0.4 pu at 0.6 s. (e) Response of rotor flux of DFIM for step change in T_{em} from −0.4 pu to 0.4 pu at 0.6 s. (f) Rotor speed response of DFIM for step change in T_{em} from −0.4 pu to 0.4 pu at 0.6 s. (g) Response of rotor currents of DFIM for step change in T_{em} from −0.4 pu to 0.4 pu at 0.6 s.

The torque produced by the DFIM follows as closely as the reference torque, which indicates good tracking behavior of the proposed control scheme comparative to classical DTC (not expressed in p.u. value), it can be seen in **Figure 4(b)**.

Stator flux and rotor flux responses of DFIM are shown in **Figure 4(c)** and **(d)** respectively. From the **Figure 4(c)** and **(d)**, it is observed that the variation in torque command is not having any influence on the stator and rotor fluxes of DFIM.

Figure 4(e) shows the rotor speed response of DFIM. From the **Figure 4(e)**, it is observed that there is continuous variation in rotor speed; of course, this variation is

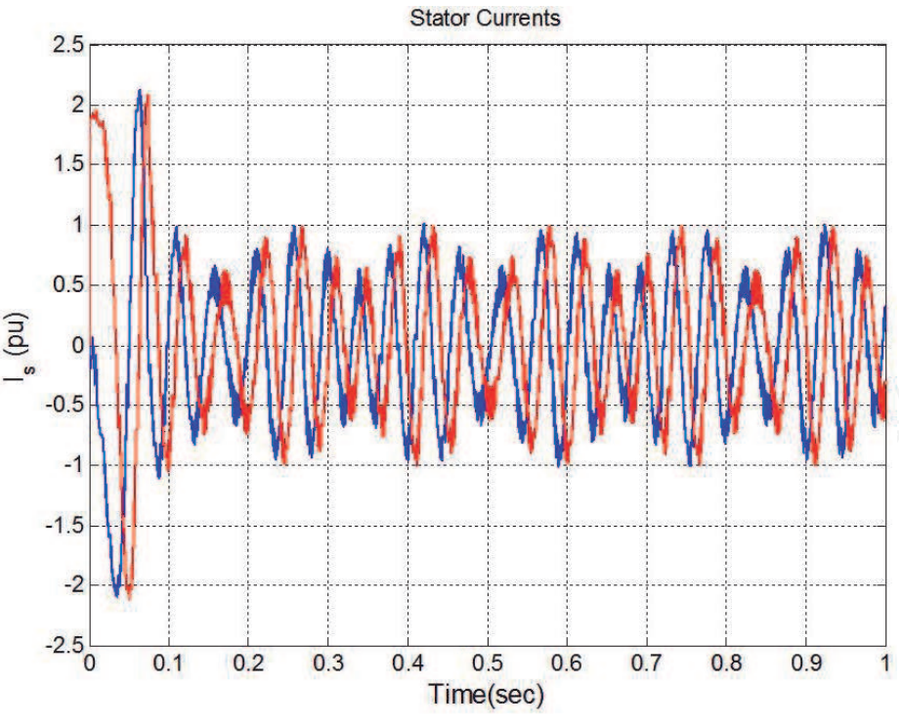
Stator Currents
I_s (pu)
Time(sec)

(a)

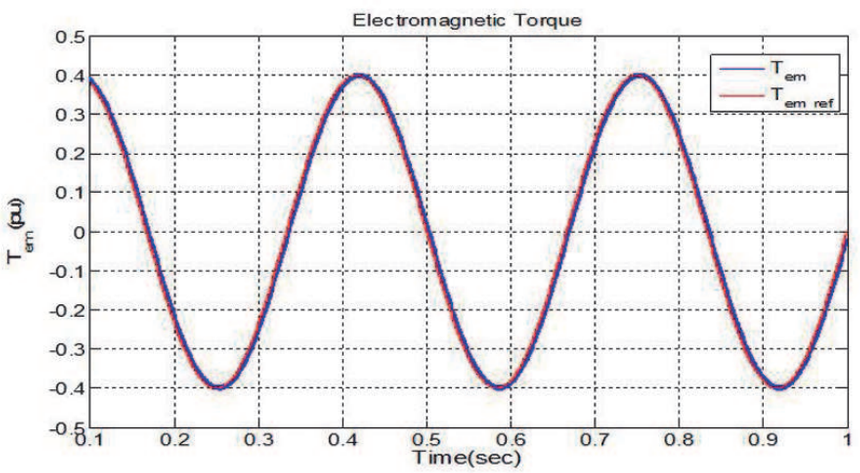
Electromagnetic Torque
T_{em}
$T_{em\ ref}$
T_{em} (pu)
Time(sec)

(i)

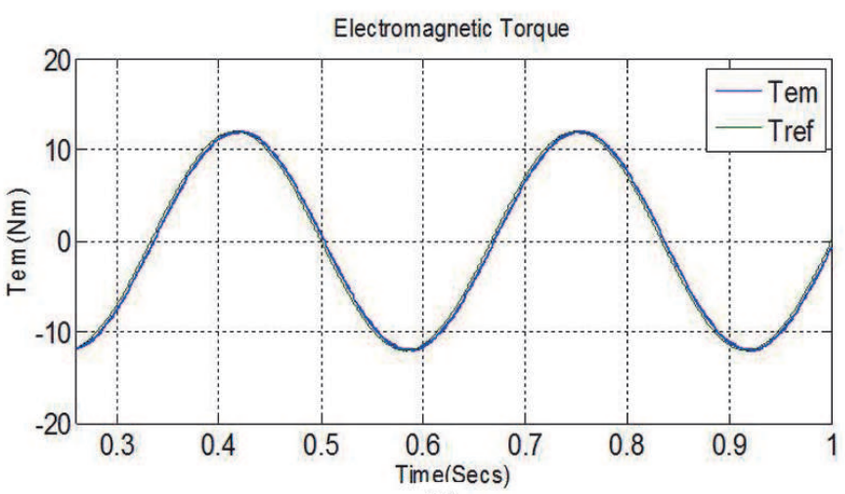
Electromagnetic Torque
Tem
Tref
Tem (Nm)
Time(Secs)

(ii)

(b)

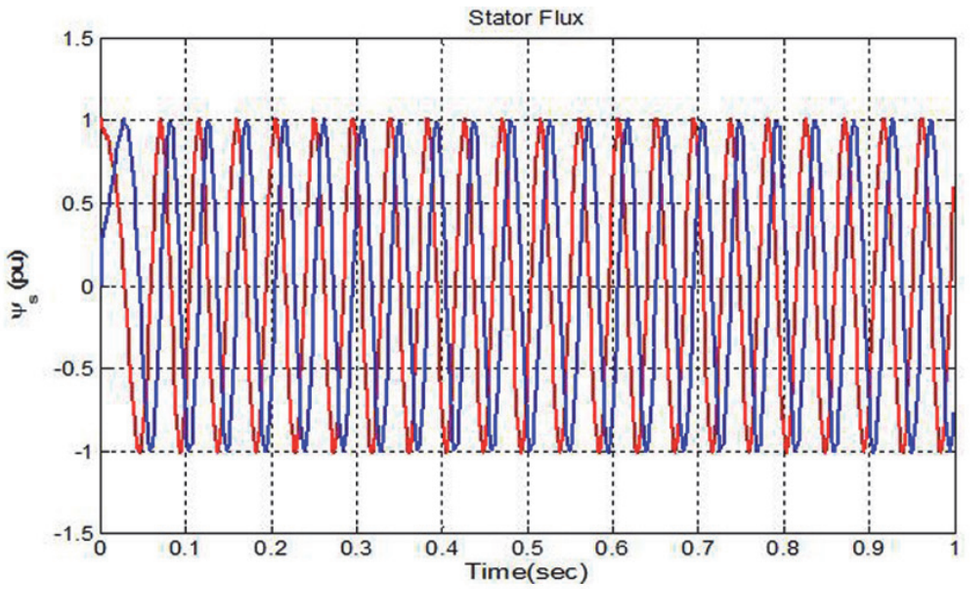
Stator Flux
ψs (pu)
Time(sec)

(c)

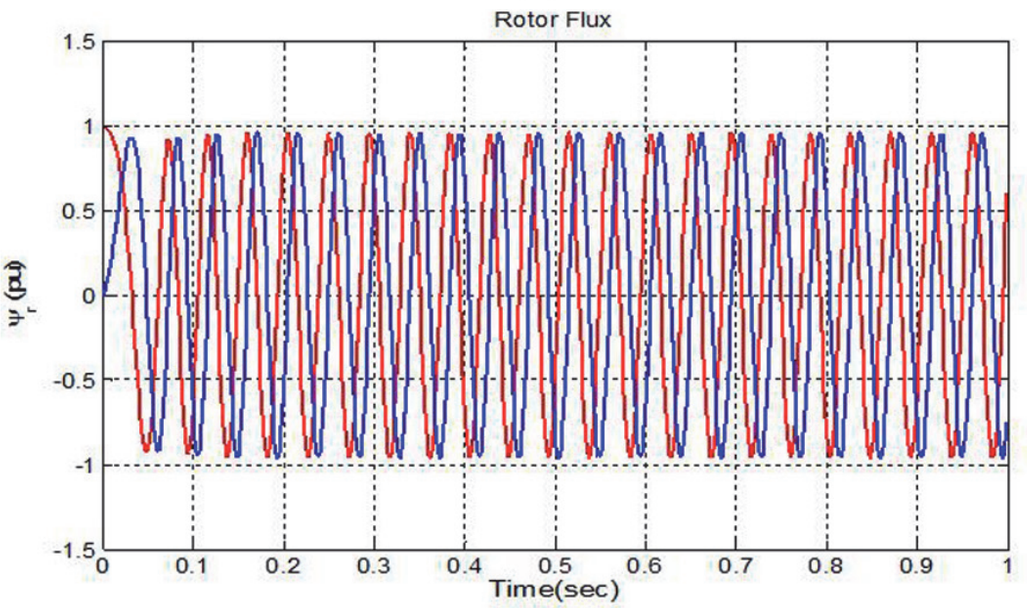
Rotor Flux
ψr (pu)
Time(sec)

(d)

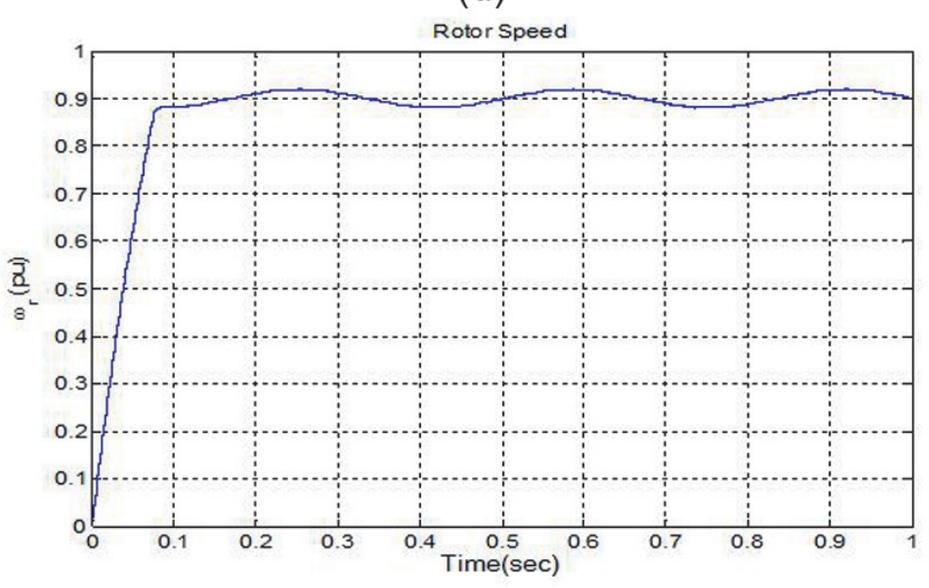
Rotor Speed
ωr (pu)
Time(sec)

(e)

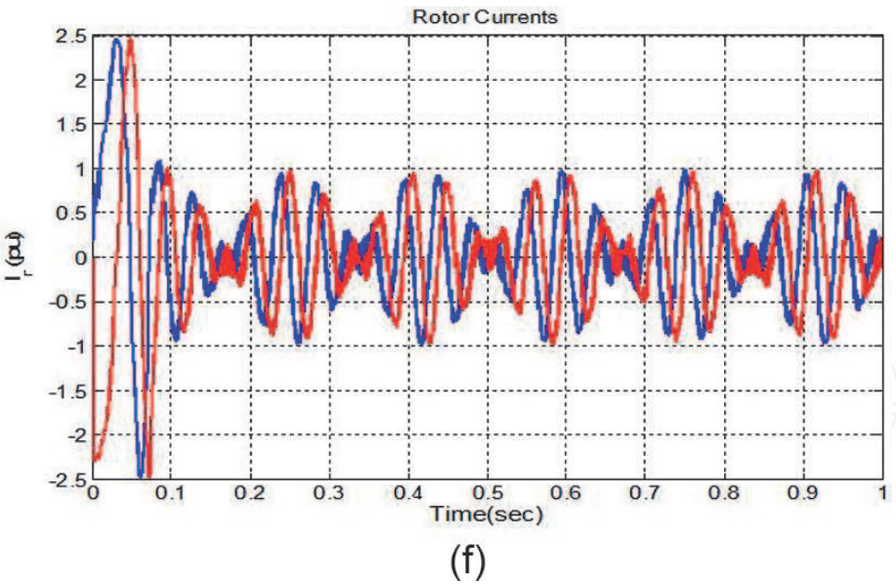

Figure 4.
(a) Response of stator currents of DFIM with variable torque command. (b) Response of developed torque of DFIM with variable torque command (i) proposed strategy (ii) classical DTC. (c) Response of stator flux of DFIM with variable torque command. (d) Response of rotor flux of DFIM with variable torque command. (e) Response of rotor speed of DFIM with variable torque command. (f) Response of rotor currents of DFIM with variable torque command.

very small it is because of variable torque command, but practically rotor speed almost constant.

The predictive DTC strategy has good tracking behavior and it is confirmed that the reduction in torque and flux ripples is achieved as there are absolute absence of over currents and reduced ripples in rotor currents as shown in **Figure 4 (f)**. From the **Figure 4(f)**, it is noticed that there is continuous increase and decrease in the amplitude of rotor currents, similar to stator currents as shown in **Figure 4(a)**.

5.3 Performance of DFIM near synchronous speed

In this Section, the performance of the proposed control scheme of DFIM has been investigated near the synchronous speed. This is examined by varying the speed of DFIM from 1580 rpm (hyper synchronous value) to 1340 rpm (sub synchronous value) in terms of sine wave with frequency of 3 rads^{-1} and phase shift of 90°, with the reference values of torque and rotor flux are set to 0.4 pu and 1 pu respectively.

Even when the speed command is varied suddenly from hyper synchronous value to sub synchronous value no much transient peaks occur in stator currents, as shown in **Figure 5(a)**, which clearly emphasizes there is reduction in over currents in stator and this is because of proper selection of switching sequence of rotor voltage vectors.

As shown in **Figure 5(b)**, the torque developed by the machine for proposed strategy and classical DTC and it closely follows the reference torque which means the dynamic performance of the machine is quite satisfactory but when the rotor speed nears the synchronous speed at around 0.5 s, variable torque ripple is produced. This variability in the torque ripple is due to continuous selection of zero voltage vectors at that instant. It indicates, the smaller amplitude of rotor voltage

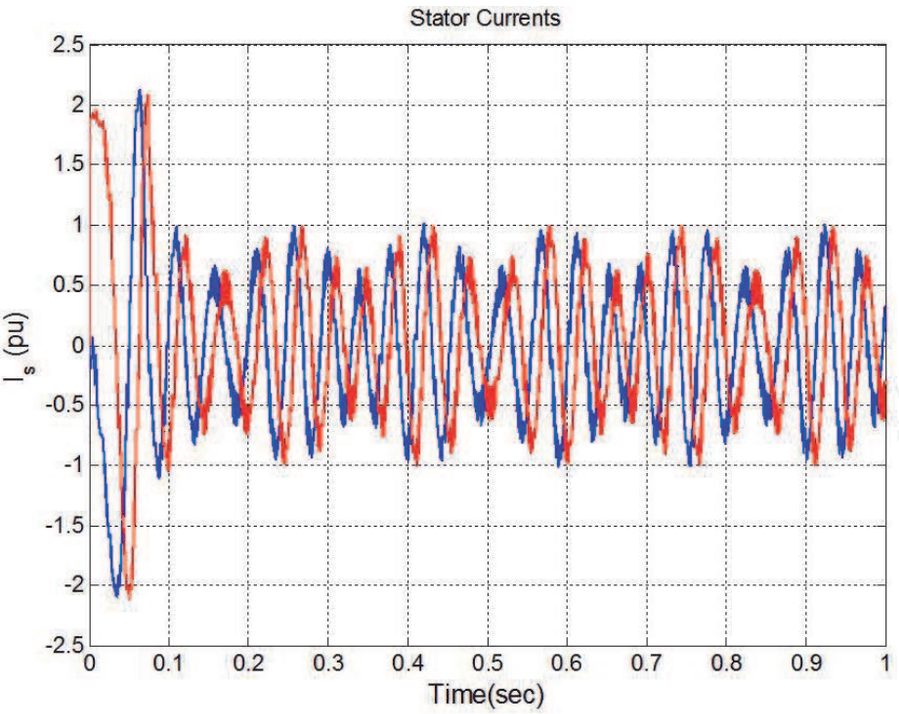
Stator Currents
I_s (pu)
Time(sec)

(a)

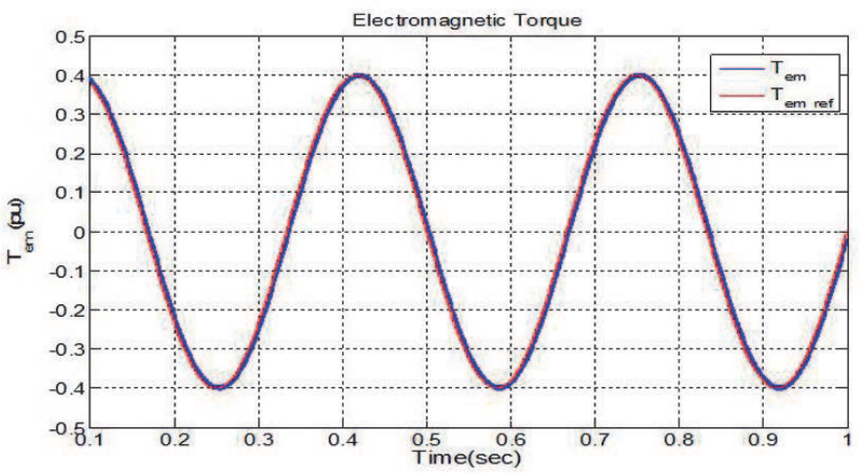
Electromagnetic Torque
T_{em}
$T_{em\ ref}$
T_{em} (pu)
Time(sec)

(i)

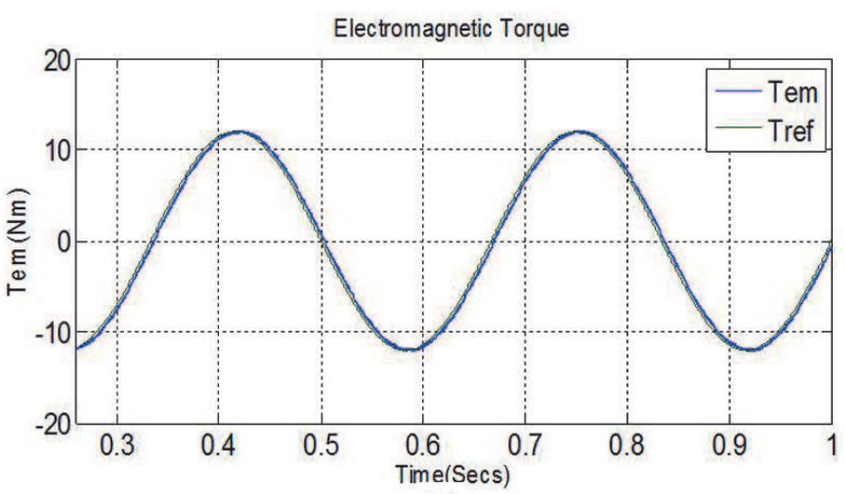
Electromagnetic Torque
Tem
Tref
Tem (Nm)
Time(Secs)

(ii)

(b)

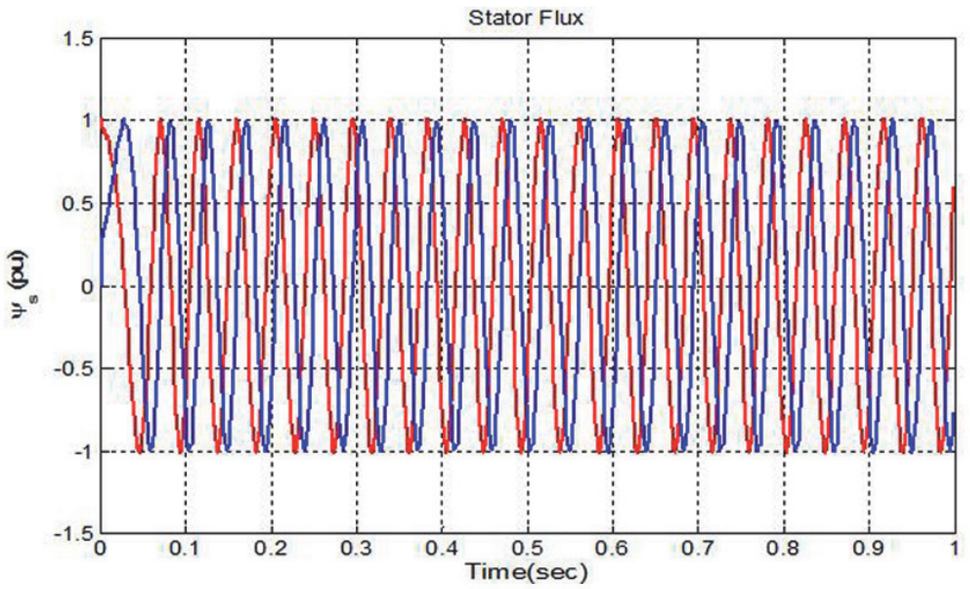
Stator Flux
ψs (pu)
Time(sec)

(c)

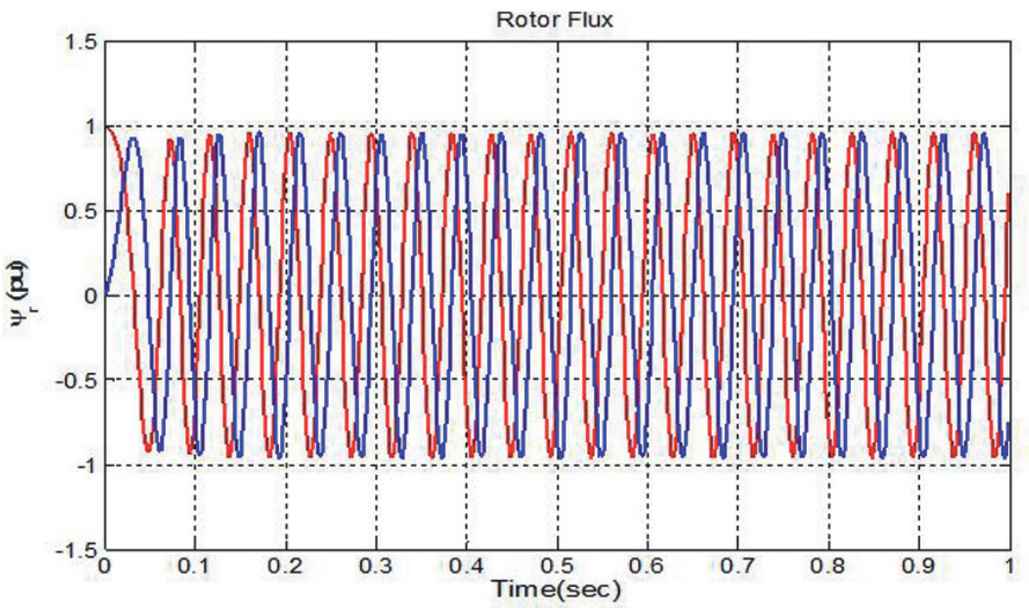
Rotor Flux
ψr (pu)
Time(sec)

(d)

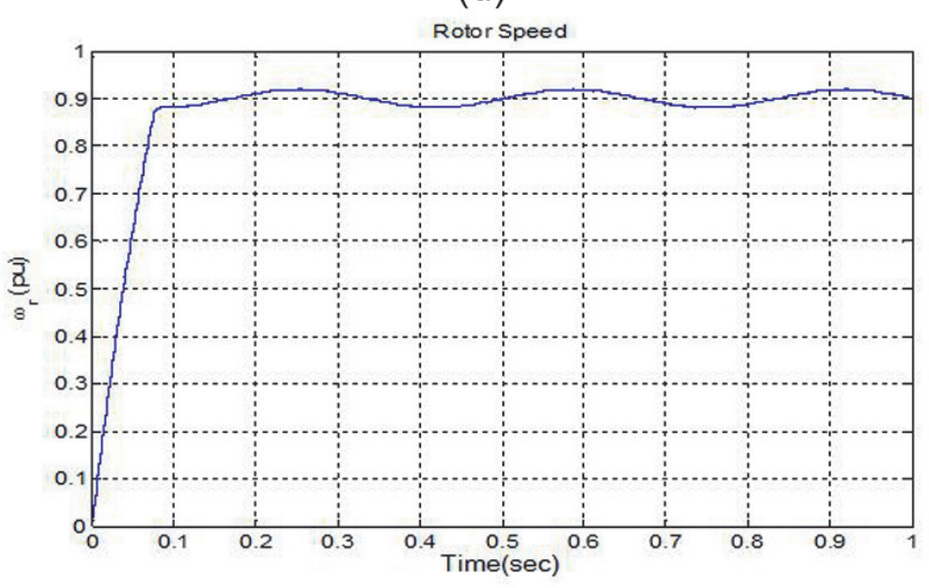
Rotor Speed
ωr (pu)
Time(sec)

(e)

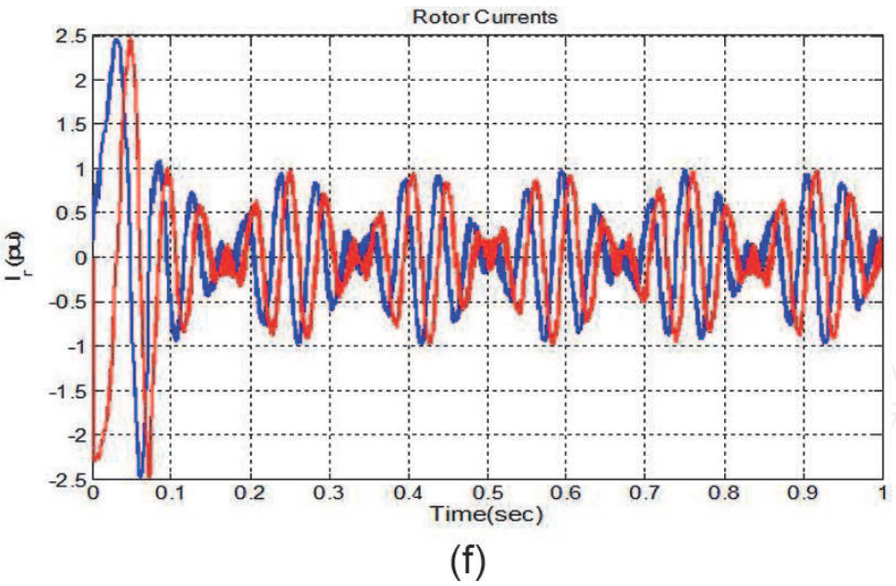

Figure 5.
(a) Response of stator currents of DFIM with variation in rotor speed from 1580 to 1340 rpm. (b) Torque response of DFIM with variation in rotor speed from 1580 to 1340 rpm (i) proposed strategy and (ii) classical DTC. (c) Response of stator flux of DFIM with variation in rotor speed from 1580 to 1340 rpm. (d) Response of rotor flux of DFIM with variation in rotor speed from 1580 to 1340 rpm. (e) Rotor speed of DFIM with variation in rotor speed from 1580 to 1340 rpm. (f) Response of rotor currents of DFIM with variation in rotor speed from 1580 to 1340 rpm.

vector is required at the instant of rotor speed nearing the synchronism, which actually causes the reduction in torque ripple and this leads to degradation of quality of control. As shown in **Figure 5(b)**, the ripples are reduced in electromagnetic torque response.

Stator flux responses are shown in **Figure 5(c)**. From the figure, it is observed that the stator flux remains constant and is not affected by change in rotor speed and also it is sinusoidal in nature.

The response of rotor flux is shown in **Figure 5(d)**, from the figure, it is observed that there is no effect on the rotor flux due to sudden change in the rotor speed and rotor flux is also not affected by the changeover.

The response of rotor speed is as shown in **Figure 5(e)**, when reference speed is varied from hyper synchronous value to sub-synchronous value and it is observed that the rotor speed response of DFIM follows the command speed.

Similar to stator currents as shown in **Figure 5(a)**, no much transient peaks occur in rotor currents, as shown in **Figure 5(f)**, that is, there is reduction in over currents in the rotor, which is because of proper selection of switching sequence of rotor voltage vectors.

6. Conclusions

The proposed control method makes two general contributions to the predictive control techniques. Firstly, it shows that using instead of two voltage vectors operating three appropriate vectors, allows operating at low constant switching frequency. Secondly, it is crucial to achieve the whole good performance of the DFIM, in terms of torque and current ripples by reducing the ripples of both directly controlled variables instead of only one.

From the proposed control method, it is possible to reduce the stress of the switching devices of the voltage source converter, in terms of low constant

switching frequency behavior and switching power losses reduction, often demanded requirements in high power applications.

It presents good tracking behavior, capable of working at variable speed operation conditions, for both motoring and generating modes at sub- synchronous and hyper synchronous speeds when compared to DTC technique, making this control suitable for applications such as wind power generation.

The new DTC technique allows obtaining quick dynamic responses in respect to DTC method, with absolute absence of non-desired over currents in the machine. It ensures reduced torque and flux ripples, due to the control effect. The simulation results showed the effectiveness of the proposed method, to control the torque and the flux of the DFIM at considerably low constant switching frequency.

7. Summary

In this Chapter, new predictive DTC has been developed for DFIM. The proposed control scheme uses two voltage vectors instead of three voltage vectors and it allows operating at low constant switching frequency and reduces torque and flux ripples, and also capable of working at variable speed operating conditions for both motoring and generating modes at sub-synchronous and hyper synchronous speeds compared to classical DTC technique. The comparison of torque and flux ripple values (difference of maximum to minimum ripple value) and its reduction given by the difference of maximum value and minimum value to average value is given in the **Table 5** below.

S. No.	Parameter	Classical DTC scheme	Predictive DTC scheme
1	Torque ripple	0.3 pu	0.01 pu
2	Reduction in torque ripple	2.5%	1.25%
3	Rotor flux ripple	0.018 pu	0.01 pu
4	Reduction in rotor flux ripple	1.8%	1.05%

Table 5.
Torque and flux ripple reduction comparison.

Author details

Gopala Venu Madhav[1*] and Y.P. Obulesu[2]

1 Department of EEE, Anurag Group of Institutions, Ghatkesar, TS, India

2 School of Electrical Engineering, VIT University, Vellore, Tamilnadu, India

*Address all correspondence to: venumadhav.gopala@gmail.com

References

[1] Blaschke F. A new method for the structural decoupling of a.C. induction machines. In: Proc. IFAC Conf., Dussesldorf, Germany, October 1971. 1971. pp. 1-15

[2] Takahashi I, Ohmori Y. High-performance direct torque control of an induction motor. IEEE Transactions on Industry Applications. 1989;**IA-25**(2): 257-264

[3] Depenbrock M. Direct self-control (DSC) of inverter-fed induction machine. IEEE Transactions on Power Electronics. 1988;**PE-3**(4):420-429

[4] Flach E, Hoffmann R, Mutschler P. Direct mean torque control of an induction motor. In: Proc. EPE'97 Conf. 1997. pp. 672-677

[5] Casadei D, Serra G, Tani K. Implementation of a direct control algorithm for induction motors based on discrete space vector modulation. IEEE Transactions on Power Electronics. 2000;**15**(4):769-777

[6] Kang JK, Sul SK. New direct torque control of induction motor for minimum torque ripple and constant switching frequency. IEEE Transactions on Industry Applications. 1999;**35**(5): 1076-1086

[7] Martins CA, Roboam X, Meynard TA, Carvalho AS. Switching frequency imposition and ripple reduction in DTC drives by using a multilevel converter. IEEE Transactions on Power Electronics. 2002;**17**(2): 286-297

[8] Sarasola I, Poza J, Rodríguez MA, Abad G. Predictive direct torque control of brushless doubly fed machine with reduced torque ripple at constant switching frequency. In: Proc. IEEE ISIE'07 Conf. 2007. pp. 1074-1079

[9] Aurtenechea S, Rodríguez MA, Oyarbide E, Torrealday JR. Predictive control strategy for dc/ac converters based on direct power control. IEEE Transactions on Industrial Electronics. 2007;**54**(3):1261-1271

[10] Pena R, Clare JC, Asher GM. Doubly fed induction generator using back-to-back PWM converters and its application to variable speed wind-energy generation. IEE Proceedings—Electric Power Applications. 1996;**143**: 231-241

[11] Gomez SA, Amenedo JLR. Grid synchronization of doubly fed induction generators using direct torque control. In: Proc. IEEE IECON'02 Conf. 2002. pp. 3338-3343

[12] Datta R, Ranganathan VT. Direct power control of grid-connected wound rotor induction machine without rotor position sensors. IEEE Transactions on Power Electronics. 2001;**16**(3):390-399

[13] Abad G, Rodríguez MA, Poza J. Predictive direct power control of the doubly fed induction machine with reduced power ripple at low constant switching frequency. In: Proc. IEEE ISIE'07 Conf. 2007. pp. 1119-1124